Vδ1 T Cells Integrated in Full-Thickness Skin Equivalents: A Model for the Role of Human Skin–Resident γδT Cells

JID Open

Natascha Andrea Kuenzel[1], Jochen Dobner[1], Doreen Reichert[1], Andrea Rossi[1], Petra Boukamp[1,2,3] and Charlotte Esser[1,3]

Vδ1 T cells are a subpopulation of γδT cells found in human dermis. Much less is known regarding their role and function in skin health and disease than regarding the roles of murine skin–resident γδT cells. In this study, we report the successful integration of Vδ1 T cells into long-term fibroblast-derived matrix skin equivalents. We isolated Vδ1 T cells from human blood, where they are rare, and established conditions for the integration and maintenance of the freshly isolated Vδ1 T cells in the skin equivalents. Plated on top of the dermal equivalents, almost all Vδ1 T cells migrated into the dermal matrix where they exerted their influence on both the dermal equivalents and the epithelium. Vδ1 T cells contributed to epidermal differentiation of HaCaT cells as indicated by histology, expression of epidermal differentiation markers, and RNA-sequencing expression profile. When complemented with the carcinoma-derived SCC13 cells instead of HaCaT, our data suggest a role for Vδ1 T cells in slowing growth of the tumor cells, as indicated by reduced stratification and changes in gene expression profiles. Together, we demonstrate the successful establishment of human Vδ1 T cell–competent skin equivalents and skin carcinoma equivalents and provide evidence for molecular and functional consequences of the Vδ1 T cells on their respective environment.

Keywords: γδT cells, Human immunocompetent skin model, Immune surveillance, Squamous cell carcinoma, Vδ1 T cells

Journal of Investigative Dermatology (2025) **145,** 1407–1421; doi:10.1016/j.jid.2024.08.037

INTRODUCTION

Skin serves as a barrier organ that guards against infections, chemicals, or UVR-induced cell damage. Skin is a complex tissue, composed of epidermis, dermis, and hypodermis. Immune cells, both resident and incoming upon infections or damage, are an integral part of skin health. In particular, skin-resident γδT cells are crucial for maintaining barrier homeostasis and function, detect DNA damage, and eliminate cancer cells (Jameson and Havran, 2007; Sumaria et al, 2011; Toulon et al, 2009). Nonmelanoma skin cancer, basal cell carcinomas, and cutaneous squamous cell carcinomas (SCCs) are the most common tumors (Madan et al, 2010). Cutaneous SCCs, in particular, are of outstanding importance not only because they are numerous and their number is still steadily increasing but also because they generate metastatic lesions, and they contribute to a high morbidity and mortality rate in the general population worldwide (Gjersvik et al, 2023).

Despite the large number of DNA-damaged cells in the skin, especially in elderly subjects (Brown et al, 2017; Jonason et al, 1996; Martincorena et al, 2015), the number of skin carcinomas is still far below what would be expected if all mutant cells would progress to carcinoma. Thus, it is not only the number of UV-induced genetic aberrations that is responsible for skin cancer progression, but it is also suggested that the immune system plays an important role. Cutaneous SCCs are typical senile tumors, emerging when the immune system's power declines with aging. Moreover, immunosuppressed patients, regardless of age, have a 65–200-fold increased risk of developing numerous and even more aggressive SCCs with a metastasis rate of up to 10% (eg, Adami et al [2003], Berg and Otley [2002], and Bordea et al [2004]). This strongly points to the importance of the immune system in controlling skin carcinogenesis.

A central role in the skin immune response was ascribed to the 2 skin-resident cell types of the innate immune system: the Langerhans cells and a subpopulation of γδT cells (T cells whose TCR consists of a γ and a δ chain [Nguyen and Soulika, 2019]), the dendritic epidermal T cells (DETCs) in mice, and Vδ1 T cells in humans. Langerhans cells take up antigens and bring them into the draining lymph nodes to activate αβ TCR-bearing T cells. On the other hand, γδT cells act directly on site as essential regulators of local immune surveillance (Dalessandri et al, 2016). They recognize cellular deregulation (wounding) and (pre)malignant

[1]IUF – Leibniz Research Institute for Environmental Medicine, Düsseldorf, Germany; and [2]German Cancer Research Centre, Heidelberg, Germany

[3]These authors contributed equally as senior authors.

Correspondence: Charlotte Esser, IUF – Leibniz Research Institute for Environmental Medicine, Auf'm Hennekamp 50, Düsseldorf 40225, Germany. E-mail: Charlotte.Esser@iuf-duesseldorf.de

Abbreviations: BM, basement membrane; DE, dermal equivalent; DETC, dendritic epidermal T cell; FBS, fetal bovine serum; MHC, major histocompatibility complex; SCC, squamous cell carcinoma; SCE, skin cancer equivalent; SE, skin equivalent

Received 27 March 2024; revised 25 June 2024; accepted 12 August 2024; accepted manuscript published online 9 October 2024; corrected proof published online 2 November 2024

© 2024 The Authors. Published by Elsevier, Inc. on behalf of the Society for Investigative Dermatology. This is an open access article under the CC BY-NC-ND license (http://creativecommons.org/licenses/by-nc-nd/4.0/).

keratinocytes and are actively involved in restoring tissue homeostasis (Jameson et al, 2002; MacLeod and Havran, 2011). Most of this knowledge is derived from mouse skin, where important immunosurveillance functions are provided by the epidermal γδT cells, the so-called DETCs. These include restoring tissue homeostasis and recognition/removal of malignant keratinocytes and melanocytes. DETCs are generated during a short time window in the fetal thymus and migrate into the skin around birth. DETCs express NKG2D receptor and the keratinocytes NKG2D ligands (Wensveen et al, 2018). In conventional in vitro cultures, the DETCs were able to kill skin carcinoma cells through a corresponding NKG2D-sensitive mechanism (Vantourout and Hayday, 2013).

In addition, human skin harbors γδT cells, mainly Vδ1 T cells, with the capability to kill melanoma skin cancer cells (Cordova et al, 2012; Cruz et al, 2018; Lo Presti et al, 2017). However, in human skin, these Vδ1 T cells predominantly reside in the dermis (Bos et al, 1990; Elbe et al, 1996). It is still unclear whether the human dermal Vδ1 T cells are produced in the fetal thymus, similar to murine DETCs. Alternatively, they might be produced throughout life and immigrate into the skin continuously. Because γδT cells (including Vδ1) are also found in the blood in minor fractions, some level of exchange with the periphery must be assumed. Today, there is no doubt that the Vδ1 T cells can be functionally analogous to DETCs (Bos et al, 1990; Toulon et al, 2009). However, lack of phenotypic similarities and their dermal predominance raises questions on the extent of equivalency with DETCs, especially regarding a mode of action not relying on direct contact.

In general, γδT cells recognize their antigen independently of major histocompatibility complex (MHC) presentation and appear specialized in recognizing stress molecules (Davey et al, 2018; Melandri et al, 2018; Sanz et al, 2023). In humans, γδT cells have 2 major subpopulations, which differ using either the Vδ1 or the Vδ2 gene segment for the variable region of the δ chain of the TCR. Vδ2 T cells (most of them also have the Vγ9 variable chain and, therefore, are often referred to as Vγ9 cells) are mainly found in the blood, where they make up about 1−10% of leukocytes. They can expand greatly and migrate into inflamed skin as a result of certain bacterial or parasitic infections. On the other hand, there are only few Vδ1 T cells in the blood but many in the dermal layer of the skin (Ebert et al, 2006).

Studies with γδT cells isolated from human skin showed that they have cytotoxic capacities and could robustly kill melanoma cells (Pang et al, 2012; Toia et al, 2019). Indeed, an intratumoral γδT cell signature proved to be the most favorable prognostic marker in a study of 39 different tumor types, including melanoma (Gentles et al, 2015; Girard et al, 2019). It is, however, noteworthy that some γδT cells, in particular, those secreting IL-17, can also act as drivers for tumor development and progression by releasing immunosuppressive cytokines or by inhibiting the antitumor effects of other T cells through PD-1/PD-L1 interaction (Raverdeau et al, 2019).

Important and useful tools to establish the functional consequences of human Vδ1 T cells are 3-dimensional skin equivalents (SEs), comprising dermis-like and epidermal layers. Most frequently, hydrogel-based SEs are used, where the keratinocytes are grown on a collagen matrix with integrated fibroblasts (Moon et al, 2021). Regarding immune cell integration in such models, beyond Langerhans cells (Bechetoille et al, 2007; Ouwehand et al, 2011), so far, macrophages (Michielon et al, 2020) and preactivated peripheral T cells were used (Huth et al, 2024; Scheurer et al, 2024; van den Bogaard et al, 2014), whereas skin-resident, nonactivated T cells have yet to be analyzed. Indeed, the majority of available SEs simply approximated immune activity by adding cytokines, most likely missing important aspects of immunosurveillance, such as cell−cell or cell−matrix interactions, to identify damage, or relevant noncytokine effectors such as chemokines, insulin-like GF, and more (Moon et al, 2021). Furthermore and as a major drawback, these models commonly suffer from poor stability, along with a limited life span (Muffler et al, 2008). To overcome such issues, we recently developed collagen-independent 3-dimensional full-thickness skin models, where normal human dermal fibroblasts isolated from adult skin established an authentic dermal matrix, either on a scaffold (scaffold-based SEs) or scaffold-free (fibroblast-derived matrix SEs) basis (Berning et al, 2015; Boehnke et al, 2012; Pavez Loriè and Boukamp, 2020; Stark et al, 2004). These models allow cultivating normal and transformed keratinocytes for several months and are highly sensitive for modulatory influences (Sobel et al, 2015; Tham et al, 2022). On the basis of the fibroblast-derived matrix SEs, in this study, we report the successful integration of freshly isolated Vδ1 T cells. We demonstrate that in this ex vivo model, the human Vδ1 T cells established almost exclusively in the dermal equivalent (DE), where they contributed to an altered expression profile of both the dermal and epidermal compartment. Thereby, they contributed to improved epidermal differentiation when performing SEs with the nontumorigenic HaCaT keratinocytes and to counteract (slow down) growth when the carcinoma-derived SCC13 cells were propagated as skin cancer equivalents (SCEs).

RESULTS

Isolation of Vδ1 T cells from buffy coats

Vδ1 T cells are a small subpopulation of γδT cells in the blood (they are rare themselves, with about 4% of lymphocytes being γδT cells). On average, the fraction of Vδ1 T cells was well below 1% in the PBMCs isolated from buffy coats of 29 different donors (Figure 1a and b). The majority of Vδ1 T cells expressed NKG2D, a sensor of tumor cells and stressed cells (Jelenčić et al, 2017; Nielsen et al, 2015; Wrobel et al, 2007), and about <20% expressed the tissue retention and activation marker CD69 (Marshall et al, 2019; Sanz et al, 2023; Temchura et al, 2005).

We successfully sorted these rare Vδ1 T cells from the PBMCs with anti-Vδ1 antibodies and magnetic cell sorting (Figure 1c). In agreement with reports from the literature (Sanz et al, 2023), the percentage of Vδ1 T cells isolated from buffy coats varied. Depending on the frequency determined for the respective donor and sorting efficacy, the percentage of the Vδ1 cells reached 35−99%. The fraction of Vδ1 T cells incorporated into the different SEs varied from a purity of 43−99%. Importantly, the magnetic sorting procedure did

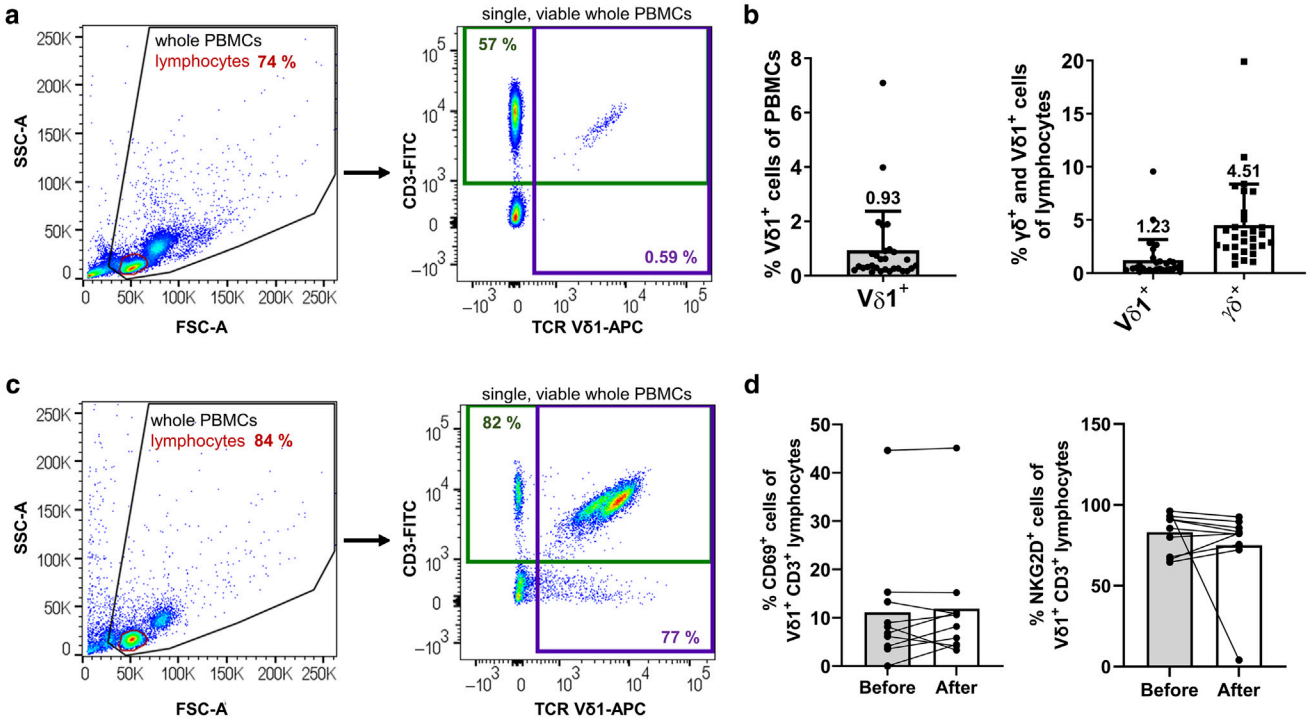

Figure 1. Purification of Vδ1 T cells. **(a)** PBMCs were isolated from human buffy coats by gradient centrifugation and stained for CD3 and Vδ1. Lymphocytes were gated according to scatter characteristics (left dotplot: small red gate in black PBMC gate; % lymphocytes of whole PBMCs [black gate]). In the example shown, 0.59% of PBMCs were $V\delta1^+$ (violet rectangle), and 57% (green rectangle) were $CD3^+$ T cells. **(b)** Frequencies of Vδ1 T cells in PBMCs (left bar graph) and for all γδT cells in lymphocytes across n = 29 different donors (right bar graph). The mean percentage is indicated for each bar. **(c)** Analysis of magnetically enriched Vδ1 T cells. A typical example is shown: 82% of cells within the whole PBMC scatter gate (left dotplot) were $CD3^+$, and 77% were $V\delta1^+$ (right dotplot, green or violet gates). **(d)** Expression of the surface markers CD69 and NKG2D (CD314) on $CD3^+$ $V\delta1^+$ cells within the lymphocyte scatter gate before the magnetic enrichment process (before) and within the positive fraction (after). n = 10 different donors. FSC-A, forward scatter area; SSC-A, side scatter area.

not affect the expression of the activation marker NKG2D or CD69 (Figure 1d), suggesting that sorting did not aberrantly activate the Vδ1 T cells. It has been described that it is possible to expand Vδ1 T cells with a complex cytokine mix (Almeida et al, 2016). However, when we tested components of this cytokine mix on our SEs, we found that it was detrimental for the integrity, particularly of the epithelial layer, and that this was independent of the presence or absence of the Vδ1 T cells (Supplementary Material SI-1). Therefore, we did not follow up on the addition of T cell–supporting cytokines further.

Integration of Vδ1 T cells into SEs and its effects on epithelial organization

We utilized our previously described fibroblast matrix–derived SEs (Berning et al, 2015) to establish the human skin Vδ1 T cell–competent SEs. For doing so, Vδ1 T cells were freshly isolated for each experiment. The successful integration of Vδ1 T cell populations from several different donors into SEs strongly supports the robustness and interindividual reproducibility of these Vδ1 T cell–competent SEs (Figure 2 [donor I] and Supplementary Material SI-2 [donors II–IV]). Each experiment consisted of 2–3 controls (SEs without T cells) and 2–3 SEs with Vδ1 T cells from the same donor (SEs with T cells). Because each SE develops its complex tissue individually, this allowed us to control also for interexperimental reproducibility.

Vδ1 T cells were applied either together with the HaCaT cells or by seeding 10^5 Vδ1 T cells onto the preformed DEs, followed by seeding of HaCaT cells 24 hours later. After 2–3 days of growth under submerged conditions, the cultures were airlifted and propagated for another 10 days before being harvested. Because step-wise application proved preferential in preliminary experiments with murine DETCs (Supplementary Material SI-5), all experiments shown in this study were performed accordingly.

To follow the distribution of the Vδ1 T cells within the SEs, cryosections were stained with a T cell–specific antibody (anti-CD3), thereby demonstrating that only few $CD3^+$ cells were present within the epithelium, whereas the vast majority of the $CD3^+$ cells had colonized within the DE (Figure 2a). Staining also demonstrated that the $CD3^+$ cells were not evenly distributed within the DEs; instead, we found grouped as well as single $CD3^+$ cells in some sections, whereas in other sections, $CD3^+$ cells were rare or even lacking (Figure 2b). Importantly, the number of $CD3^+$ cells showed no significant quantitative differences in different SEs built with Vδ1 T cells from the same donor. Although plated evenly on top of the DE, our finding of an irregular homing suggests that migration of the Vδ1 T cells into the DE is not a passive falling down but likely reflects a directed migratory process. In addition, we analyzed the $CD3^+$ cells from SEs for their Vδ1 receptor status by flow cytometry. Cells with

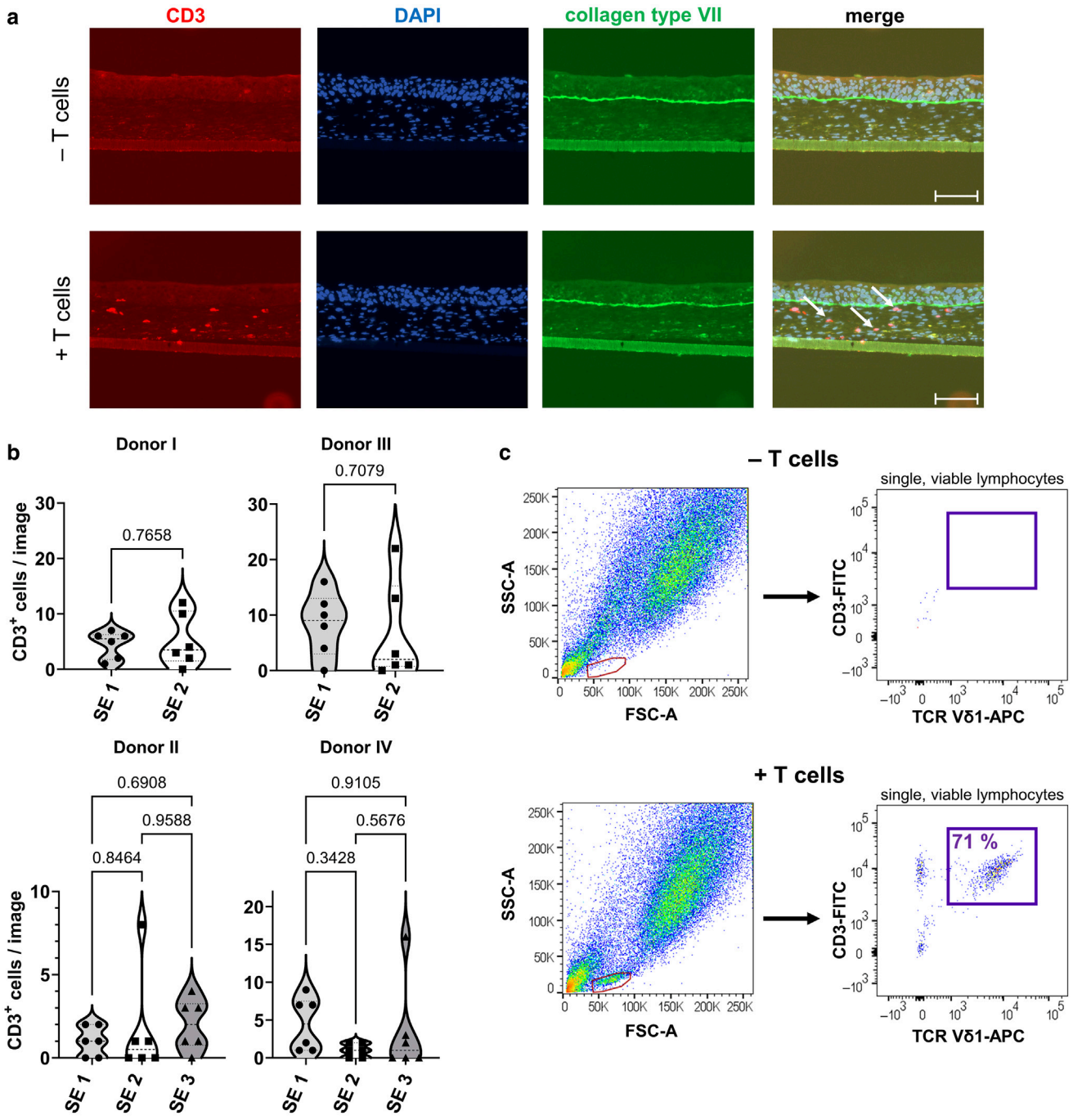

Figure 2. Vδ1 T cells migrate into the dermis and survive for at least 14 days after seeding. Immunofluorescence confirmation and FACS quantification of Vδ1 T cells in the SEs were performed. Vδ1 T cells were isolated and seeded onto a dermal equivalent built from human fibroblasts 1 day before seeding of HaCaT cells, followed by air lifting 2–3 days later. In the example shown in **a** and **c**, on the day of seeding, 79 % of single, viable PBMCs were Vδ1$^+$ cells. Fourteen days after Vδ1 T cell seeding (ie, 13 days after HaCaT seeding), the SEs consisted of the dermal equivalent covered with a stratified epithelium. **(a)** Immunofluorescence staining to show the presence and localization of T cells (green: collagen type VII, to highlight the border between epithelium and dermal equivalent underneath; blue: DAPI staining for nuclei; red: anti-CD3). Arrows point to CD3$^+$ cells. Bar = 100 μm. **(b)** Number of CD3$^+$ cells per image taken. Results of Vδ1 T cells from 4 independent donors are shown. Two individual SEs for donors I and III and 3 individual SEs for donors II and IV were analyzed each. CD3$^+$ cells were counted per image, and each dot in the plots represents the data of 1 immunofluorescent image, that is, 6 data points per SE are shown in the violin plots. Quantification for donors I and III was analyzed with students *t*-test; for donors II and IV, 1-way ANOVA was used. *P*-values are given above the graphs; none of them were significant. **(c)** Fourteen days after Vδ1 T cell seeding, SEs were harvested and digested, and single-cell suspensions were stained for flow cytometric analysis. A representative example is shown. In the Vδ1 T cell–containing SEs, a distinct cell population was observed (absent in controls), with scatter characteristics typical for lymphocytes (red gate). Within this population, 71% were double stained for CD3$^+$ Vδ1$^+$. FCS-A, forward scatter area; SSC-A, side scatter area; SE, skin equivalent.

typical lymphocyte scatter characteristics were present only in models with T cells (Figure 2c). The vast majority of these cells (see red gate) (Figure 2c) were Vδ1$^+$ CD3$^+$ T cells, demonstrating that the Vδ1 T cells remained viable and that TCR remained positive during the 2-week observation period.

In conclusion, Vδ1 T cells established and survived in our SEs without the addition of T cell–specific cytokines, demonstrating that all essential factors are provided by the fibroblasts and keratinocytes in the SEs. Importantly, in all experiments, the majority of the Vδ1 T cells moved into the dermal matrix, suggesting for a similar specific homing of the human Vδ1 T cells in our experimental model as in human skin. Finally, the results were reproducible with Vδ1 T cells from different donors, thereby supporting the feasibility and relevance of this approach.

Functional and molecular consequence of integrating Vδ1 T cells into the human HaCaT SEs

Comparing tissue morphology/organization of the Vδ1 T cell–containing versus control SEs, we found evidence for improved epithelial organization and differentiation, as indicated by histology (Figure 3a) and further confirmed by staining for the early (keratin 10) and late (FLG) epidermal differentiation markers (Figure 3c and d). Keratin 10, expressed throughout a largely unstructured epithelium in the control SEs (without T cells), was preferentially seen in the suprabasal layers (as typical for normal epidermis) of the better stratified epithelium in the presence of Vδ1 T cells (Figure 3c). Similarly, expression of FLG was increased in the uppermost layer of the epithelium, as also indicated by semiquantification of the FLG expression in 10 samples each with and without Vδ1 T cells (Figure 3d, violin plots). Development of the basement membrane (BM) did not seem to be affected. The BM component collagen type VII was similarly expressed in the control and Vδ1 T cell–containing SEs, evident by continuous lining of the BM zone (Figures 2a and 3b). Thus, the Vδ1 T cells obviously provoked improved stratification and differentiation of the HaCaT epithelium.

For murine DETCs, orientation of the dendrites toward the stratum corneum is supposed to signal the barrier status of the epidermis (Chodaczek et al, 2012). Most human Vδ1 T cells lack direct contact with the keratinocytes; thus, contribution to epidermal differentiation likely results from Vδ1 T cell–induced GF and/or cytokine-based communication.

Vδ1 T cells modulate gene expression in the epithelium and DEs of HaCaT SEs

We next determined the role of Vδ1 T cells on the expression profile in the epidermal and dermal compartment by performing comparative RNA-sequencing analysis from HaCaT SEs with and without Vδ1 T cells. Three individual SE using T cells from the same donor were sequenced, thus avoiding interpersonal variation of the Vδ1 T cells. We separated the HaCaT epithelium from the DE and isolated RNA from the 2 compartments independently before being subjected to RNA sequencing. An important first observation was that many genes were differentially up and downregulated in both the epithelium and the DEs when Vδ1 T cells were present (Figure 4a and d). A total of 93 and 101 genes were significantly differentially expressed (with T cells vs without T cells) in the epithelium and DE, respectively, when choosing a $P = .05$.

Gene expression changes in the HaCaT epithelium. Concerning gene regulation in the HaCaT epithelium, the most strongly upregulated genes were *VHL*, *ZNF430*, *MAUS3*, *MSL2*, *KEAP1*, *IRX3*, and *BTBD3*. These genes involve ubiquitin ligation, transcription, and DNA binding, indicative for processes of ongoing cell activation. In addition, we found moderate upregulation of differentiation-associated genes. Although below the significance threshold, expressions of genes such as kallikreins 6, 12, and 13; *LORICRIN*; *HRNR*; and *IVL* as well as several *SPRR* and *EDC* genes were increased in the HaCaT epithelium when Vδ1 T cells were present in the DE (Figure 4b, volcano plot), thereby further supporting the effect of the Vδ1 T cells on epidermal differentiation. The highest-ranking pathways in a gene ontology analysis of the HaCaT epithelium indicated defense responses, in particular.

Gene expression changes in the DEs. In the DEs, on the other hand, many immune-related genes were upregulated, with some reaching a >3-fold upregulation (Figure 4d). In particular, we found *CCL4*, *CCL5*, and *CCL13* as well as *CXCL9* and *CXCL11* to be upregulated upon Vδ1 T cell integration (Figure 4e, volcano plot). These proteins have chemoattractant activity for leukocytes, memory T helper cells, and eosinophils; thus, they have a role in accumulation of leukocytes during inflammation (Griffith et al, 2014). This coincides with the gene ontology results, which indicate defense and response to cytokines as well as neutrophil chemotaxis (Figure 4f). *GZMA* and *PD-1*, known to be expressed by Vδ1 T cells (Holling et al, 2004; Wrobel et al, 2007; Wu et al, 2022), were upregulated, and in addition, *HLA-DR* and MHC class II–associated invariant chain peptide (*CD74* or *CLIP*), the MHC class II chaperone protein, were more prominent in the Vδ1 T cell–containing DEs. We verified selected genes (*GZMA*, *PD1*, *CCL13*) by RT-qPCR and could confirm their significant upregulation in the DEs containing Vδ1 T cells (Supplementary Material SI-3).

In conclusion, our RNA-sequencing data emphasize that the Vδ1 T cells influence the expression profiles of the epidermis-forming keratinocytes as well as of the cells in the DEs, the dermal fibroblasts, and themselves. This further suggests that the Vδ1 T cells condition the microenvironment and, with that, complement the mutual epidermal–dermal interaction in this tissue context.

Effects of Vδ1 T cells on epithelia formed by the skin carcinoma–derived SCC13 cells

We finally asked for the consequence of Vδ1 T cells when being exposed to skin carcinoma cells in SEs. To generate SCEs, the skin SCC cell line SCC13 (Rheinwald and Beckett, 1981) was plated on DEs, either without (control) or with preseeded Vδ1 T cells. Because the SCC13 cells have proven to be highly invasive, that is, quickly invade into the DE when plated at high density (Berning et al, 2015), we complemented the SCEs with only low numbers (5×10^2 up to maximally 1×10^4 per SCE) of SCC13 cells, thereby promoting the establishment of only superficially growing tumor epithelia (Figure 5a). In the presence of the skin carcinoma cells, the Vδ1 T cells successfully integrated in the DE (Figure 5b), as they did when being cocultured with HaCaT cells, thereby strengthening our hypothesis that dermal homing is an intrinsic trait of the human Vδ1 T cells. Similar to that in the SEs, the number of $CD3^+$ cells per microscopic

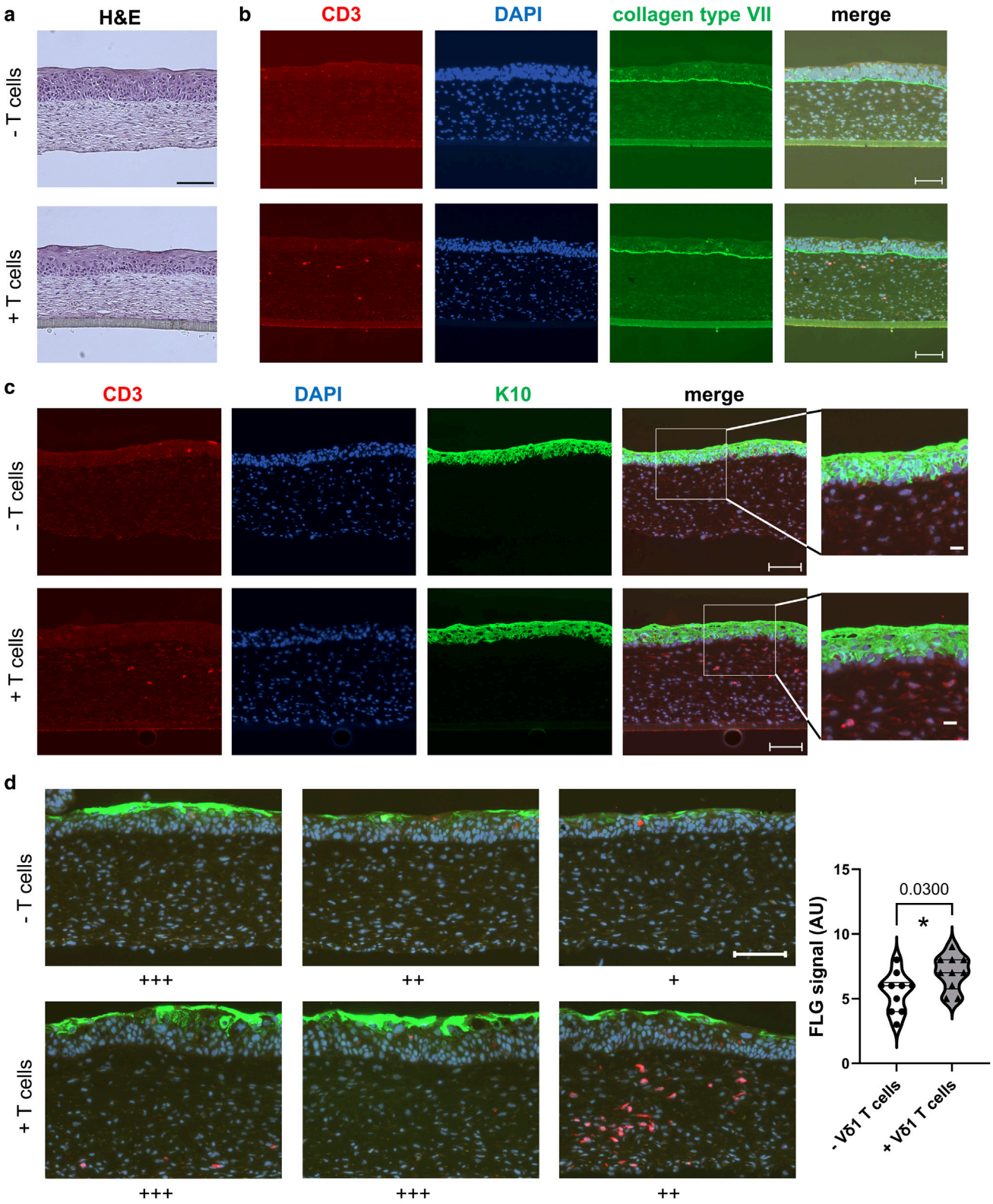

Figure 3. Vδ1 T cells present in the dermis positively affect epithelial differentiation. Histological structure and expression of different epithelial marker proteins were analyzed in SEs without or with T cells. In the experiment shown, on day of seeding, 77% of single, viable PBMCs were Vδ1$^+$ cells. Fourteen days after T cell and 13 days after HaCaT seeding, the SEs had formed an epidermal epithelium and were harvested (27−35% of single, viable cells with scatter characteristics typical of lymphocytes represented a CD3$^+$ Vδ1$^+$ double-positive population in the dermal compartment at day of harvest). **(a)** H&E staining of skin models in the presence or absence of Vδ1 T cells. The lower, brighter region of the SE represents the DE, whereas the upper, darker part shows the epithelium. Bar = 100 μm. **(b)** Immunofluorescence assay for collagen type VII (green), DAPI (blue), CD3 (red). The organization of the nuclei in the epithelium differs between the samples with and without T cells. Bar = 100 μm. **(c, d)** Epithelial differentiation markers upon T cell integration (green: K10 [for **c**] or FLG [for **d**], blue: DAPI, red: CD3). **(c)** In SEs without T cells, K10 is expressed throughout a largely unstructured epithelium, whereas in the presence of Vδ1 T cells,

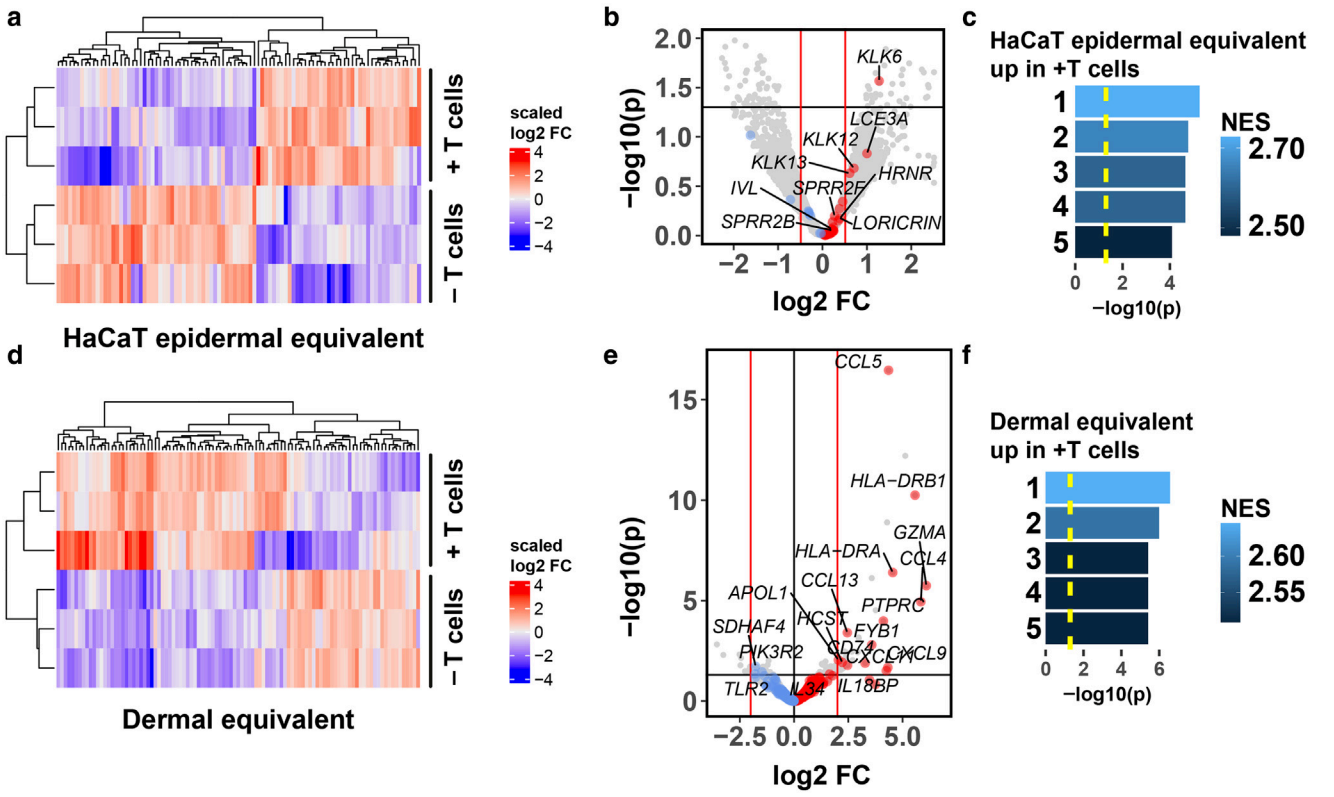

Figure 4. Gene expression profiling of SEs with or without Vδ1 T cells. RNAseq data from HaCaT (**a**–**c**) epidermal equivalent and (**d**–**f**) dermal equivalent separated from 3 individual SEs supplemented with Vδ1 T cells from 1 donor (purity of Vδ1 T cells was 77% of PBMCs at day of seeding). **(a)** Heatmap of the differentially expressed genes in the 3 HaCaT epithelia. Red indicates higher expression, and blue indicates lower expression when comparing epithelia from SEs with Vδ1 T cells (+T cells) with those without (−T cells). **(b)** Volcano plot showing up/downregulation of genes in HaCaT epithelia. Red dots indicate upregulated genes, and blue dots indicate downregulated genes when Vδ1 T cells are present. Typical genes of epidermal differentiation are indicated. For visualization, values have been winsorized to a max −log10(p) of 2 and absolute $\log_2$ FC of 2.5. **(c)** Highest pathways in GO analysis: numbers refer to (1) response to biotic stimulus, (2) immune response, (3) response to external biotic stimulus, (4) response to other organism, and (5) defense response. **(d)** Heatmap and (**e**) volcano plot showing selected genes of the biological process immune, and GO analysis of the dermal equivalents. (**f**) Highest upregulated pathways: numbers refer to (1) immune response, (2) immune system process, (3) response to biotic stimulus, (4) response to external biotic stimulus, and (5) biological process involved in interspecies interaction between organisms. FC, fold change; GO, gene ontology; NES, normalzed enrichment core; RNAseq, RNA sequencing; SE, skin equivalent.

image taken varied within the same SCE, again reflecting that $CD3^+$ cells are not evenly distributed throughout the SCE. However, when we quantified the number of $CD3^+$ cells across several images, there was no significant difference between the number of $CD3^+$ cells in different SCEs built with Vδ1 T cells from the same donor (Figure 5c). When comparing the total numbers of $CD3^+$ cells in SCC13 SCEs with those from HaCaT SEs, we found a significant reduction of $CD3^+$ cells in the SCC13 SCEs (Figure 5d). Because all culture conditions were kept identical, a response to the different keratinocytes seems possible for this discrepancy.

When investigating SCEs with the lowest concentration (5×10^2) of SCC13 cells, growth of the tumor epithelium was very similar. Both without and with Vδ1 T cells, the often discontinuous epithelium consisted of only 1 up to at most 3 cell layers (data not shown). With increasing number of SCC13 cells (5×10^3 and 1×10^4), multilayered epithelia had formed within the 2 weeks. However, compared with the controls (without T cells), overall thickness of the epithelia appeared reduced when Vδ1 T cells were present. Accordingly, quantification of the size of the epithelia showed reduced thickness in 2 of 3 independent experiments (SCC13 SCEs with Vδ1 T cells from 3 different donors and 2–3 individual SCEs for each donor), thereby suggesting some growth-restricting activity of the Vδ1 T cells on the SCC13 cells in this tissue-like environment (Supplementary Material SI-4).

The SCC13 cells expressed collagen type VII under both conditions, but in contrast to HaCaT SEs, the protein was not deposited at the BM zone (data not shown). Earlier

K10 expression predominates suprabasally in the more orderly structured epithelium (see also magnified inserts). Bars = 100 and 20 μm. **(d)** The level of the late differentiation marker FLG is increased when Vδ1 T cells are present. For quantification, 3 images per SE were analyzed for 4 independent donors and assigned to a category: − indicates no FLG-stained regions, + indicates few faintly stained regions, ++ indicates strongly stained discontinous regions, and +++ indicates intensely stained continuous FLG^+ layer. Values of all 3 images/SE were summed up and are depicted as 1 data point. Images of 2 SEs of donor IV are shown as examples. Bar = 100 μm. Values were plotted without and with Vδ1 T cells (n = 10 SEs each), accordingly. Statistical significance was established using Students *t*-test, $*P < .05$. DE, dermal equivalent; K10, keratin 10; SE, skin equivalent.

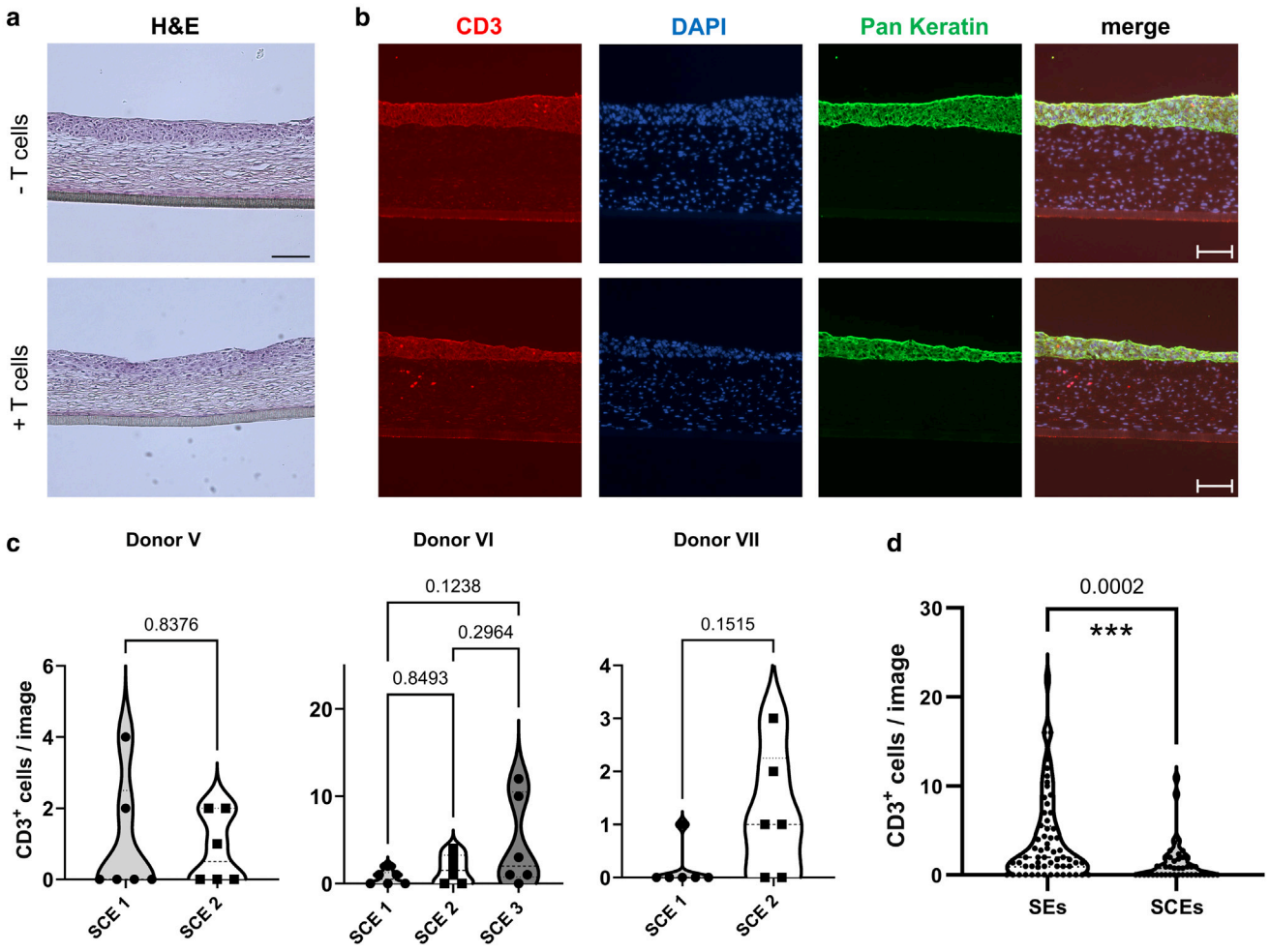

Figure 5. Vδ1 T cells successfully integrate into SCC13 carcinoma cell containing SCEs. SCEs were performed with Vδ1 T cells from 3 different donors (donors V, VI, and VII) and with 2 or 3 individual SCEs for each donor. Each SCE was analyzed for its morphological appearance (histology), epithelial nature of the SCC13 epithelium (immunofluorescence staining for pan-keratin), and distribution (CD3) and number (quantification) of the $CD3^+$ T cells. In the experiment shown, 93% of single, viable PBMCs were $V\delta1^+$ on day of seeding, and 43–55% of single, viable lymphocytes were $CD3^+$ $V\delta1^+$ double positive at the time of harvest (14 days after T cell seeding) in the 3 SCEs. **(a)** H&E-stained histological section of an SCE sample in the absence (−T cells, upper panel) and presence of Vδ1 T cells (+ T cells, lower panel). Bar = 100 μm. **(b)** IIF of the SCEs for CD3 to mark the Vδ1 T cells, DAPI to mark all nuclei, pan-keratin to mark the SCC13 epithelium, and the overlay (merge) of all stainings. Similar to HaCaT SEs, also in SCC13 SCEs, the $CD3^+$ cells were unevenly distributed and largely restricted to the DE. Bar = 100 μm. **(c)** Quantification of the number of $CD3^+$ cells per image. For each SCE, the $CD3^+$ cells in 6 images were counted. Results shown are from 2 independent SCEs with Vδ1 T cells from donors V and VII and 3 independent SCEs with Vδ1 T cells from donor VI (utilized in **a** and **b**). Students *t*-test was used for the analysis of the $CD3^+$ cells from donor V, Mann–Whitney test was used for donor VII, and 1-way ANOVA was used for donor VI. **(d)** Comparison of the number of $CD3^+$ cells in HaCaT SEs versus SCC13 SCEs. The total number of $CD3^+$ cells from HaCaT SEs (10 SEs from 4 different donors and 6 images per SE; n = 60 images) was compared with that from SCC13 SCEs (7 SCEs from 3 different donors and 6 images per SCE; n = 42 images). Values were normalized against the total number of seeded cells (varied between 0.72 and 1.15 × 10^5). For statistical analysis, the Mann–Whitney test was used. Note the significant difference in cell maintenance in HaCaT SEs versus SCC13 SCEs. ***$P < .001$. DE, dermal equivalent; IIF, indirect immunofluorescence; SCE, skin cancer equivalent; SE, skin equivalent.

experiments had shown that collagen type VII and laminin-332 are expressed also by the SCC13 cells in SCEs and remain largely unstructured (Berning, 2015; Berning et al, 2015). Together, this demonstrates that the tumor cells are able to express the different BM components, but a structured BM is not established in this context.

Molecular consequence of integrating Vδ1 T cells into SCC13 SCEs

To obtain further insight into a potential antitumor effect of Vδ1 T cells, we performed RNA-sequencing analyses from the SCC13 SCEs. Whereas HaCaT cells form a coherent epithelium, cell–cell coherence of the SCC13 cells is poorly developed. Accordingly, the epithelia formed by the SCC13 cells proved to be less compact/stable, thereby preventing clear separation of tumor epithelium and DE. Hence, RNA-sequencing analyses were performed from RNA of the entire SSC13 SCEs. Again, the presence of Vδ1 T cells resulted in differential gene expression of numerous genes (Figure 6a). Top upregulated genes (according to the *P*-values) were *CCL18*, *RNAse1*, *CCL13*, *CD52*, *SPP1*, *TOP3B*, and *CXCL10*.

To track down differentially expressed genes that might point to Vδ1 T cell specificity, we compared the expression profiles of the SCC13 SCEs (with T cells) with those from the DEs of the HaCaT SEs (with T cells). Interestingly, we found 8

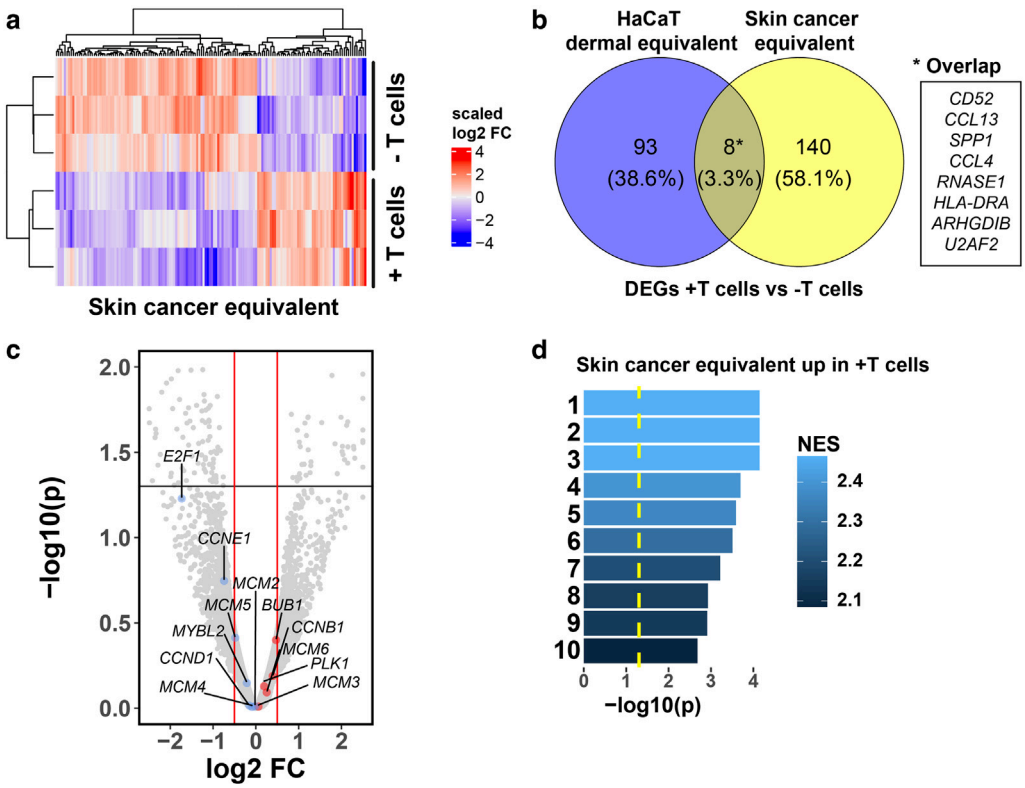

Figure 6. Gene expression profiling of skin cancer equivalents with or without T cells. RNAseq analysis was performed from 3 biological replicates of SCC13 SCEs with Vδ1 T cells from the same donor (purity of Vδ1 T cells was 93% of PBMCs at day of seeding and 43−55% of lymphocytes at day of harvest) and 3 controls (SCC13 SCEs without Vδ1 T cells). **(a)** Heatmap of DEGs in the individual SCEs. Red indicates higher expression, and blue indicates lower expression in models with T cells than in those without T cells. **(b)** Venn diagram comparing DEGs ($P \leq .05$, $\log_2$ FC >1.5) from the DE of the HaCaT SEs (dermal compartment) (Figure 4 provides details) with the SSC13 SCEs (dermal and epidermal part combined). **(c)** Volcano plot showing genes belonging to the cancer-specific signature (Whitfield et al, 2006). For visualization, values have been winsorized to a max −log10(p) of 2 and absolute $\log_2$ FC of 2.5. (**d**) Gene set enrichment analysis of the SCC13 SCEs with Vδ1 T cells compared with those without (control): (1) response to biotic stimulus, (2) response to external biotic stimulus, (3) response to other organism, (4) biological process involved in interspecies interaction between organisms, (5) defense response, (6) defense response to other organism, (7) response to external stimulus, (8) innate immune response, (9) cell surface receptor signaling pathway, and (10) immune response. DE, dermal equivalent; DEG, differentially expressed gene; FC, fold change; RNAseq, RNA sequencing; SCE, skin cancer equivalent; SE, skin equivalent.

genes that were differentially expressed in both the SCC13 SCEs and DEs of the HaCaT SEs and thus suggestive for a general but minor Vδ1 T cell−dependent regulatory unit (Figure 6b). Apoptotic processes, indicative for active tumor cell killing, were not found in the SSC13 SCEs. However, a tumor-specific proliferation-associated gene signature was described previously, whose expression was correlated with tumor cell proliferation rates (Whitfield et al, 2006). This proliferation-associated gene signature included the cell cycle transcriptional regulator *E2F1*, the replication-initiation complex proteins *MCM2−6* as well as *MYBL2*; the serin/threonine-protein kinases *BUB1* and *PLK1*; and cyclins *CCNE1*, *CCND1*, and *CCNB1*. Interestingly, several of these genes (*E2F1*; *MCM2*, *4*, and *5*; *MYBL2*; *CCNE1*; and *CCND1*) were downregulated in SCC13 SCEs containing Vδ1 T cells (Figure 6c). Thus, it is tempting to suggest that their downregulation, in particular, the downregulation of *E2F1* and *CCNE1*, may have slowed growth of the SCC13 cells and may thus explain reduced stratification (thinner epithelium) of the SCC13 epithelia when Vδ1 T cells were present. Gene set enrichment analysis of the RNA-sequencing data additionally indicated that multifold processes were upregulated in the presence of the Vδ1 T cells (Figure 6d), suggestive for an active stress stimulus and inflammatory response.

In conclusion, the Vδ1 T cells significantly influence the gene expression pattern of the SCEs built with the SCC-derived SCC13 cells by creating an expression profile indicative of stress and inflammation and may, in addition, contribute to tumor surveillance by reducing/slowing down tumor cell proliferation.

DISCUSSION

Animal models, although important and essential, are not in all cases suitable for understanding regulatory cues in human tissues. In particular, skin is highly divergent in mouse and man, making human organotypic culture models most worthwhile. Accordingly, the development of 3-dimensional full-thickness skin models, also termed SEs, has fundamentally contributed to our understanding of composition and structure (epidermis and DE), cell−cell interactions between the 2 compartments, and cell signaling required for a normal homeostatic skin. Complemented with tumor cells, the SCEs also serve as excellent models to study the requirements for

skin cancer initiation and progression (Berning et al, 2015; Ratushny et al, 2012).

Different models exist regarding the composition of the DE. In our hands, the fibroblast-derived matrix-based SEs have proven most favorable and robust (Pavez Loriè and Boukamp, 2020; Tham et al, 2022). In this model, the human dermal fibroblasts generate a stable authentic dermal matrix (Boehnke et al, 2007) that allows normal and immortal skin keratinocytes to establish a well-structured and differentiated, long-lived epidermis (Boehnke et al, 2007; Stark et al, 2006) and also allows tumor cells to express their genuine phenotype (Berning, 2015; Tham et al, 2022). Because of the histological resemblance to native human skin in terms of structure and composition as well as its potential for longevity, we chose fibroblast-derived matrix-based SEs also as the in vitro platform for the integration of the human γδT cells.

Importantly, we aimed at establishing a model for the rare skin-resident Vδ1 T cells, whose function is to preserve normal skin homeostasis by interacting with and signaling to the epidermis as well as to contribute to tumor surveillance in the skin (reviewed in Cruz et al [2018] and Toulon et al [2009]). Although our present knowledge concerning skin-resident γδT cells is mostly derived from studies with mouse skin harboring dendritic T cells in the epidermis, the DETCs (MacLeod and Havran, 2011; Strid et al, 2009), data with human skin–resident Vδ1 T cells are rare, and in particular, tissue-related studies are still missing (Qu et al, 2022).

We now describe the development of a human Vδ1 T cell–competent SEs and report on a role of the Vδ1 T cells in tissue homeostasis and control of skin carcinoma cells. We demonstrate the successful integration of Vδ1 T cells into the SEs derived from human dermal fibroblasts and HaCaT keratinocytes using sorted primary, unstimulated Vδ1 T cells from healthy donors. Remarkably, T cell growth-enhancing cytokine cocktails, commonly used for the expansion of γδT cells in vitro (Almeida et al, 2016), proved detrimental for our SEs, thereby implicating the power of self-organization and maintenance of the different skin cells in this tissue composite. Although it is possible that ficollation and antibody-mediated magnetic sorting might activate T cells, we further proved that the sorted cells retained CD69 and NKGD2 expression and thereby verified that the isolation procedure did not change expression of these 2 important surface proteins.

A first and most striking finding was the localization of the Vδ1 T cells in the SEs. Plating the Vδ1 T cells on top of the DE and overlaying them with the keratinocytes might have favored their integration within the developing epithelium. However, in all experiments, we found migration of the Vδ1 T cells into the DEs, and this was independent of being cocultured with the nontumorigenic HaCaT cells or the SCC13 skin carcinoma cells. In human skin, both αβ and γδT cells mainly reside in the dermis, with only few cells being present in the epidermis (Bos et al, 1990). Thus, our result that the Vδ1 T cells actively integrate into the DE highlights the species-specific tissue location of the human Vδ1 T cells and argues for selective/targeted communication (cross-talk) between the skin cells (fibroblasts and keratinocytes) and the Vδ1 T cells for finding their place in the skin. This interpretation is further supported by preliminary experiments with murine skin–resident γδT cells, the DETCs, which in mouse skin typically reside in the epidermis. When plated on top of the human DE, the DETCs remained as rounded cells (without dendrites) in the lower part of the HaCaT epithelium and faded away over the 10-day observation period. Thus, different from the human Vδ1 T cells, the DETCs seem to be specified for an intraepidermal location but obviously are not supported to survive in the human environment long term (Supplementary Material SI-5). Although finite presence of the DETCs correlated with improved growth of the HaCaT cells, their aberrant localization and ephemerality excluded them as relevant substitutes for the human Vδ1 T cells.

Second, we provide evidence that the human Vδ1 T cells are of functional consequence in the SEs. Mouse and human γδT cells were shown to monitor skin integrity by recognizing damaged cells (reviewed in Cruz et al [2018] and Toulon et al [2009]). Because HaCaT cells represent keratinocytes in their early transformation state—with UV-indicative genetic alterations but maintained propensity for epidermal differentiation—they appeared as an optimal choice for the establishment of the Vδ1 T cell–competent SEs and to address how Vδ1 T cells may respond to such UV-damaged cells.

Interestingly, supplementation of HaCaT SEs with Vδ1 T cells contributed to improved stratification and differentiation of the HaCaT epithelium, as indicated by histology, RNA expression profile, and immunofluorescence staining for epidermal differentiation markers. Thus, the HaCaT cells did not appear to be recognized as aberrant cells. In mice, it is suggested that DETC dendrites contacting keratinocytes allow constant sensing of the epithelial barrier status (Chodaczek et al, 2012), pointing to mechanical sensing as a regulatory principle. In our Vδ1 T cell–competent SEs, as in human skin, the Vδ1 T cells were resident mostly in the dermis and did not form dendrites. Nevertheless, they supported epidermal differentiation. This strongly argues for a Vδ1-mediated paracrine loop, as already established for dermal–epidermal interaction (Berning, 2015; Stark et al, 2004), affecting gene expression and stratification in the HaCaT epithelium.

To study Vδ1 T cells' role in tumor surveillance, we established SCEs with the human SCC13 skin SCC line (Rheinwald and Beckett, 1981). Under normal conditions (plated at high cell numbers), these cells start off as surface epithelia and later break through the BM and invade the DE (Berning et al, 2015). To delay invasion, we here limited the number of carcinoma cells, and this allowed us to provide evidence for a role of the Vδ1 T cells during this early phase of tumor growth, that is, when the carcinoma cells were still growing as surface epithelia. Although we did not find indications for apoptotic destruction of the carcinoma cells, we noticed a tendency for reduced epithelial stratification (tumor tissue height). So far, most experimental models showing skin tumor killing were performed in 2-dimensional cultures with murine DETCs and murine carcinoma or melanoma cells, where tumor cell killing required direct cell contact with the DETCs (Xiang et al, 2020). Comparing Vδ2 cells with Vδ1 cells in coculture killing assays with Daudis Burkitt lymphoma cells indicated that Vδ1 T cells can kill the tumor cells

but possibly not primarily through granzyme/perforin (Sanz et al, 2023). Studies in melanoma suggested that PD-1$^+$ Vδ1 T cells might act by retaining effector T cell responses in checkpoint inhibitor therapy (Davies et al, 2024). In this study, we provide evidence for growth restriction of the tumor epithelium in the presence of the human dermis–resident Vδ1 T cells. Because this correlates with downregulation of the tumor-specific proliferation-associated gene signature (Whitfield et al, 2006), paracrine regulation through the Vδ1 T cells is likely. Our RNA-sequencing analyses point to significant upregulation of the cytokines CCL18, CCL4, and CCL13, factors related to immunoregulation/angiogenesis, but leave the nature of tumor growth–regulatory factors still elusive. Indeed, it was unexpected that we found evidence for antitumor effects of Vδ1 T cells other than direct killing. More studies will be necessary to identify how Vδ1 T cells affect tumor growth because this is prerequisite for any clinical/therapeutic use.

To unravel a potential Vδ1 T cell gene signature, we compared the RNA-sequencing data from Vδ1 T cell–containing DEs of the HaCaT SEs with the data from the Vδ1 T cell–containing SCC13 SCEs. Although it is not possible to assign particular genes found in the the RNA-sequencing data to particular cells, even in the DEs of the HaCaT SEs (no clear differentiation between fibroblasts and Vδ1 T cells), we think it likely that the expression of some of the most highly upregulated genes have arisen from the Vδ1 T cells, that is, *CD52*, *SPP1*, *RNASE1*, *CCL4*, and *CCL13/HLA-DR*. In healthy human skin, MHC class II is present on antigen-presenting cells and some possibly preactivated T cells (Angel et al, 2007; Holling et al, 2004) but not on healthy keratinocytes. Therefore, MHC-II expression likely reflects the Vδ1 T cell presence. The finding of RNAse1 in the presence of Vδ1 T cells might indicate a beneficial downstream effect on the keratinocytes because RNAse1 is a secretory ribonuclease and can act as a tissue-protecting enzyme (Fischer et al, 2013) and is involved in innate immunity and anti-inflammation, achieving host defense and anticancer effects. In mice, RNAse1 favors an antitumor tissue microenvironment. Notably, analysis of cancer-killing potential revealed that T cell–mediated antitumor immunity was enhanced by RNAse1. These studies were done on conventional T cells, and our model will allow to test further whether similar mechanism operates in Vδ1 skin-homing T cells (Wang et al, 2023).

CD52 is widely expressed on immune cells and with immune regulatory functions (Samten, 2013), although expression on the Vδ1 T cell subset has not been demonstrated specifically. It is currently unknown how activity of Vδ1 T cells might be therapeutically supported or strengthened in the skin, and our model should well be suited to study this further. Furthermore, our model will permit to study also the effects of Vδ1 T cells upon DNA damage of the skin (eg, by UVR) or in response to pathogenic bacteria, a typical scenario in inflamed skin. Obviously, further possibilities of the model include gene ablation by, for example, CRISPR/Cas of the cells involved to identify mechanisms further.

In any case, it would be desirable to generate immortalized Vδ1 T cells, which can be propagated in vitro by genetically engineered telomerase expression to allow for easier large-scale screening and circumvent the issue of low T cell number, which can be isolated from donors.

In conclusion, we show that skin-resident Vδ1 T cells can successfully and reproducibly be integrated in human SEs and SCEs and studied for their functional and molecular characteristics. Similar to their counterparts in human skin, the freshly isolated Vδ1 T cells migrate and establish in the DEs, where they contribute to significant changes in gene expression in the dermal and epidermal layer, contribute to improved epidermal differentiation, and exert antitumor effects. Thus, this model proved useful to study Vδ1 T cells in the skin and will constitute an excellent tool to address further questions both regarding Vδ1 T cells biology and their possible therapeutic harnessing in skin cancer.

MATERIALS AND METHODS

Cell lines

We have shown previously that the fibroblast-derived matrix-based SEs represent long-term human 3-dimensional organotypic culture models that closely resemble human adult skin with its authentic dermal matrix equivalent and a perfectly stratified and differentiated epidermis, when using normal human dermal fibroblasts and skin keratinocytes (Berning et al, 2015). To query the interaction with the Vδ1 T cells, in turn, we selected for the spontaneously immortalized, nontumorigenic HaCaT cells (Boukamp et al, 1988). HaCaT cells are more dependent on external influences to exert terminal epidermal differentiation than normal keratinocytes and should be more sensitive for the Vδ1 T cell's ability to recognize and support barrier function (Davey et al, 2018). Moreover, similar to many normal keratinocytes in human UV-exposed skin, HaCaT cells contain UV-indicative *p53* mutations and cutaneous SCC-characteristic genetic alterations, albeit they are not tumorigenic (Lehman et al, 1993). Because of their altered genetics and their otherwise largely normal phenotype, they are ideal to get first insights into the role of Vδ1 T cells in immunosurveillance. To address the role of Vδ1 T cells in tumor surveillance, we selected for the skin SCC-derived SCC13 cells (Rheinwald and Beckett, 1981), which were proven to express MICA and MICB, ligands of NKG2D (Supplementary Material SI-6), and to exert their full tumorigenic potential also in fibroblast-derived matrix-based SCEs (Berning et al, 2015).

Normal human dermal fibroblasts, isolated as described previously (Pavez Lorié and Boukamp, 2020); HaCaT cells (Boukamp et al, 1988); and the SCC13 cells (Rheinwald and Beckett, 1981) were utilized to generate SEs and SCEs. Fibroblasts and HaCaT cells were cultured in DMEM plus 10% fetal bovine serum (FBS) and 1% (v/v) penicillin/streptomycin at 37 °C, 5% carbon dioxide, and 20% oxygen. SCC13 cells were cultured in 3:1 DMEM/Ham's F12 (PanBiotech) plus 5% FBS and 1 % penicillin/streptomycin. HaCaT and SCC13 cells were subcultured by treatment with 0.05% EDTA for 5 minutes followed by detachment with 0.4% trypsin. Fibroblasts were detached using 0.1% trypsin. Mycoplasm and virus contamination were excluded for all cell types by the Multiplex Cell Contamination Test (Multiplexion, German Cancer Research Centre) and the VenorGeM One Step Kit (Minerva Biolabs). HaCaT and SCC13 cell authentification was done by short tandem repeat profiling (CLS).

Isolation of Vδ1 T cells from buffy coats

Buffy coats from healthy donors were obtained on the day of donation and ficollized within 24 hours to obtain PBMCs. Erythrocytes were removed using a hypotonic buffer, and magnetic

purification of the PBMCs was done using MojoSort Human anti-Vδ1-allophycocyanin nanobeads (BioLegend), according to the manufacturer's instructions. Supplementary Material SI-7 provides a more detailed description. To verify sorting success, whole PBMCs and positive and negative fractions of the magnetic sorting procedure were used for flow cytometry staining and analysis. Donors could provide written, informed consent for the use of blood components, which were not needed for patients, in scientific research, and use of their cells was approved by the ethics committee of the Medical Faculty of the University of Düsseldorf (Düsseldorf, Germany) (registration number 2020-1260).

Depending on the donor and as determined by staining with anti-Vδ1 and anti-CD3 antibodies, Vδ1 T cell frequency was between 0.1 and 7% of the total PBMC fraction. Purity and number of the Vδ1 T cells used are indicated in the respective figure legends. We found addition of $\pm 1 \times 10^5$ per SE or SCE as a realistic and obviously sufficient number of Vδ1 T cells that can be reached in all isolations.

Flow cytometry

PBMCs were first incubated with anti-Fc receptor antibodies (BD or BioLegend) or tandem signal enhancer (Miltenyi Biotech), followed by addition of antibodies (diluted in PBS, 2% FBS, and 2 mM EDTA). Cells were stained for 15 minutes at 4 °C, washed once, and analyzed on a FACSCanto II and FlowJo, version 10.8.0, or FACS-Diva Software (BD). Dead cells and doublets were gated out according to scatter characteristics and DAPI staining. DAPI was added shortly before analysis. The percentages of cell populations shown are based on single, viable cells. Negative controls were unstained cells and isotype controls.

For separation of the dermal and epithelial compartments, SEs were enzymatically digested with 1 mg/ml Dispase II (30 minutes, 37 °C), and the epithelial layer was carefully pulled off, followed by a second digestion with 2 mg/ml collagenase P and 0.1 mg/ml DNAseI (Roche). SCEs were directly digested with these enzymes; the 2 layers could not be separated mechanically. Cell suspensions were filtered using a cell strainer and washed with PBS (+2% FBS and 2 mM EDTA) before staining and flow cytometric analysis. For a list of antibodies, Supplementary Material Table SI-8.

Generation of SE and SCE

For our basic model, we utilized fibroblast-derived matrix-based SEs, established as described previously (Berning et al, 2015). In brief, $0.4-0.5 \times 10^6$ normal human fibroblasts (passage 7–10) were seeded onto filter inserts at 1–2-day intervals in 3 successive steps (12-well ThinCert Inserts, Greiner Bio-One, Kremsmünster, Austria). For submerged cultivation, the wells and inserts were prefilled with cell-derived matrix medium—3:1 DMEM/Ham's F12 plus 10% FBS and 1% penicillin/streptomycin/amphotericin B—and additionally supplemented with 2.5 ng/ml human recombinant epidermal GF, 5 ng/ml basic fibroblast GF, 1 ng/ml human recombinant TGFβ (all from Gibco); 5 μg/ml human recombinant insulin; and freshly added 200 μg/ml 2-phospho-L-ascorbic acid-trisodium salt (Sigma-Aldrich). The fibroblasts were kept submerged for at least 3 weeks, with medium being changed twice a week. During this time, the fibroblasts developed an extracellular matrix–rich DE (Pavez Loriè and Boukamp, 2020). On the day of Vδ1 T cell isolation, the medium in the wells and inserts of the DEs was replaced by SE medium (3:1 DMEM/F12, 10% FBS, 1% penicillin/streptomycin/amphotericin B, 0.1 nM cholera toxin, 0.4 μg/ml hydrocortisone, and freshly added 200 μg/ml 2-phospho-L-ascorbic acid-trisodium salt [all from Sigma-Aldrich]). The Vδ1 T cell–enriched suspension, containing $\sim 1 \times 10^5$ cells in 500 μl SE medium, was carefully pipetted on top of DEs. Control DEs received 500 μl SE medium only. One day after Vδ1 T cell seeding, 0.5×10^6 HaCaT cells or $0.5-1 \times 10^4$ SCC13 cells (cell number as indicated in the figure legends) were added on top of the DEs. Two to 3 days after seeding of the epithelial cells, the cultures were lifted to the air–liquid interface by removing the medium from the insert. During the epithelial growth phase, the medium was changed twice a week, and the SEs/SCEs were harvested 14 days after Vδ1 T cell seeding.

For initial experiments, cytokines known to stimulate the growth of the Vδ1 T cells in vitro (Almeida et al, 2016) were added to the SE medium (100 ng/ml IL-4, 7 ng/ml IL-21, 15 ng/ml IL-1β [Miltenyi Biotech] and InvivoMAb CD3 antibody [Bio X Cell, Lebanon, NH]).

Harvest of the SEs and SCEs

At the day of harvest, the medium was removed from the cultures, and medium aliquots were stored at −80 °C. The SEs grown on top of the filter insert were cut out of the insert with a scalpel and divided into 2–3 pieces. One piece was transferred to a fixation solution for histological analysis (Morphisto) and stored in that solution for at least 24 hours before processing and embedding in paraffin. The second piece was embedded in a cryomold containing Tissue-Tek O.C.T. compound (Sakura Finetek Europe) and was snap frozen for cryosectioning and immunostaining. In some cases, a third piece was used for flow cytometric analysis or was digested with Dispase II (1 mg/ml in PBS) for 30 minutes at 37 °C to separate the dermal and epithelial compartment. Tissue of both compartments was then snap frozen and subjected to RNA isolation with standard methods, using the innuPREP RNA Mini Kit 2.0 (Innuscreen), according to manufacturer's instructions. Isolated RNA was used for RNA-sequencing analysis and RT-PCR for selected genes.

Histology and immunofluorescence

H&E staining was performed on paraffin-embedded sections (7 μm), following standard procedures. Images were taken using a DM2500 microscope equipped with a Leica DFZ450 camera and a ×10 objective. Image analysis and processing were performed using the ImageJ and Fiji softwares (Schindelin et al, 2012) with the CAi Fiji package (Center for Advanced Imaging, Heinrich-Heine-University).

Immunofluorescence staining was performed on cryosections. The sections (7 μm) were fixed in 80% methanol for 10 minutes at 4 °C and acetone at −20 °C for 2 minutes. After blocking with 3% BSA in PBS at room temperature, the primary antibodies were added (diluted in 3% BSA in PBS), and the slides were incubated at 4 °C overnight. Slides were washed once with PBS with 0.1 % Triton-X-100, 2 times with PBS, and once with water. Secondary antibodies were added (diluted in 3% BSA in PBS), and the slides were incubated for 60 minutes at room temperature. Slides were washed as described earlier and mounted with Vectashield Mounting Medium with DAPI (Vector Laboratories). Images were taken with an AxioImager.M2 microscope (Zeiss) using an AxioCam MR R3 camera and the EC Plan-Neofluar ×10/0.30 M27 objective. Negative controls were done with secondary antibody only. Images from a given experiment were counted (unblinded) on the same day to ascertain equal assessment. Image analysis and processing were performed with the Zen 3.5 software (Zeiss). The list of antibodies is provided in Supplementary Material Table SI-8.

For quantification of FLG expression, an FLG score was generated with 4 categories: −, indicating no FLG staining (0); +, indicating few faintly stained FLG+ regions (1); ++, indicating strongly stained

discontinuous FLG+ layer (2); and +++, indicating intensely stained continuous FLG+ layer. Three images per SE from all 4 donors were evaluated, and their values were summed up and plotted without and with T cells, accordingly. Statistical significance was established using Students *t*-test; $*P < .05$.

Real-time PCR

Supplementary Material Table SI-9 provides details on method of cDNA generation, amplification, and primer sequences.

RNA-sequencing analysis

Double-stranded cDNA synthesis and amplification. Total RNA integrity was assessed using a High Sensitivity RNA ScreenTape Analysis (Agilent). Only samples with an RNA integrity number equivalent ≥7 were subjected to cDNA synthesis, cDNA amplification, and preparation of the sequencing library. First-strand cDNA synthesis was performed by combining 200 ng total RNA, 2 μl 10 μM RT primer (5′ -> 3′: AAG CAG TGG TAT CAA CGC AGA GTA CTT TTT TTT TTT TTT TTT TTT TTT TTT TTT TV), 1 μl 10 mM (of each) dNTPs (Vazyme), and distilled water up to 6 μl. The reaction was incubated for 5 minutes at 70 °C. Afterward, 2.5 μl 4X Template Switching Buffer (New England Biolabs), 0.5 μl of 75 μM Template Switching Oligo (5′ -> 3′: GCT AAT CAT TGC AAG CAG TGG TAT CAA CGC AGA GTA CAT rGrGrG), and 1 μl Template Switching RT Enzyme Mix (New England Biolabs) were added. Second-strand synthesis was performed for 90 minutes at 42 °C, followed by heat inactivation for 5 minutes at 85 °C. Double-stranded cDNA was amplified for 8 cycles in two 50 μl reaction mixes per sample, each containing 10 μl double-stranded cDNA, 25 μl 2X Phanta Max Buffer (Vazyme), 1 μl 10 mM (of each) dNTPs, 2 μl 1 U/μl Phanta Max Super Fidelity Polymerase (Vazyme), 1 μl 10 μM cDNA PCR amplification primer (5′ -> 3′: AAG CAG TGG TAT CAA CGC AGA GT), and 11 μl aqua dest. A total of 8 PCR cycles were performed. One microliter of 20 U/μl exonuclease I (Thermo Fisher Scientific) was added to each reaction, incubated for 15 minutes at 37 °C, and heat inactivated for 15 minutes at 80 °C. Final products were purified using AMPure XP beads (Beckham Coulter) at a ratio of 0.8 X. Concentrations were measured on a Qubit Fluorometer (Thermo Fisher Scientific) with the high sensitivity double-stranded DNA kit (Thermo Fisher Scientific).

Sequencing library preparation and sequencing. Library preparation was performed according to the Ligation sequencing amplicons—Native Barcoding Kit 24 V14 (Oxford Nanopore Technologies, SQK-NBD114.24) according to the version NBA_9168_v114_revE_15Sep2022. Briefly, equal amounts of double-stranded cDNA were subjected to library preparation. Final libraries were quantified on a Qubit Fluorometer using the high-sensitivity double-stranded DNA kit. Library size was determined using a D1000 Screen Tape assay (Agilent). A total amount of 15 fmol of final libraries was loaded on a P2 solo flow cell and sequenced for 72 hours.

Sequencing data analysis. Basecalling was performed using the Guppy basecaller (version 6.4.6). Resulting FASTQ files were concatenated and mapped to the reference genome (GRCh38) using Minimap2 (version 2.24). All further analysis was performed using R (version 4.2.2). Sequence reads were counted using Rsubread::featureCounts (version 2.12.3) with options for long sequencing reads and GRCh38.106 to annotate transcripts. Afterward, reads were normalized to counts per million, and differentially expressed transcripts were identified using edgeR (version 3.40.2). Gene set enrichment analysis was performed using clusterProfiler::gseGO (version 4.6.2). Gene set enrichment analysis was resampled 10 times to increase accuracy. All data were visualized using ggplot2 (version 3.4.2) and ComplexHeatmap (version 2.14).

Statistics

Graphs and statistical calculations were done using Graphpad Prism software, version 10.2.0. $P < .05$ was considered significant.

DATA AVAILABILITY STATEMENT

The sequencing data have been deposited to the National Center for Biotechnology Information sequence read archive with the BioProject accession number RJNA1151223 (https://www.ncbi.nlm.nih.gov/sra/PRJNA1151223).

ORCIDS

Natascha Andrea Kuenzel: http://orcid.org/0000-0001-8885-5123
Jochen Dobner: http://orcid.org/0000-0002-6336-9716
Doreen Reichert: http://orcid.org/0000-0003-1486-9797
Andrea Rossi: http://orcid.org/0000-0001-5863-6448
Petra Boukamp: http://orcid.org/0000-0001-5155-1759
Charlotte Esser: http://orcid.org/0000-0002-2957-4636

CONFLICT OF INTEREST

The authors state no conflict of interest.

ACKNOWLEGMENTS

We thank Elizabeth Pavez-Lorie and Katharina Janke for generously sharing their expertise and the cells and Swantje Steinwachs for expert help. We would also like to thank Fabienne Ruhmöller and Jessica Nagel for contribution to pilot experiments and Mariko Palfalvi for advice on the computer language R. This work was made possible through the financial support of the Wilhelm-Sander-Stiftung (project 2020.130.1).

AUTHOR CONTRIBUTIONS

Conceptualization: PB, CE; Data Curation: JD; Formal Analysis: NAK, DR, PB, CE; Funding Acquisition: PB, CE; Investigation NAK, JD; Methodology: NAK, PB; Project Administration: CE, PB, NAK; Supervision: PB, CE; Validation: NAK, PB; Visualization: NAK, JD, DR; Resources: JD, AR; Writing — Original Draft Preparation: NAK, JD, PB, CE; Writing — Review and Editing: NAK, JD, PB, CE

SUPPLEMENTARY MATERIAL

Supplementary material is linked to the online version of the paper at www.jidonline.org, and at https://doi.org/10.1016/j.jid.2024.08.037.

REFERENCES

Adami J, Gäbel H, Lindelöf B, Ekström K, Rydh B, Glimelius B, et al. Cancer risk following organ transplantation: a nationwide cohort study in Sweden. Br J Cancer 2003;89:1221–7.

Almeida AR, Correia DV, Fernandes-Platzgummer A, da Silva CL, da Silva MG, Anjos DR, et al. Delta one T cells for immunotherapy of chronic lymphocytic leukemia: clinical-grade expansion/differentiation and preclinical proof of concept. Clin Cancer Res 2016;22:5795–804.

Angel CE, George E, Ostrovsky LL, Dunbar PR. Comprehensive analysis of MHC-II expression in healthy human skin. Immunol Cell Biol 2007;85:363–9.

Bechetoille N, Dezutter-Dambuyant C, Damour O, André V, Orly I, Perrier E. Effects of solar ultraviolet radiation on engineered human skin equivalent containing both Langerhans cells and dermal dendritic cells. Tissue Eng 2007;13:2667–79.

Berg D, Otley CC. Skin cancer in organ transplant recipients: epidemiology, pathogenesis, and management. J Am Acad Dermatol 2002;47:1–17.

Berning M. Three-dimensional in vitro skin and skin cancer models based on fibroblast-derived matrix dissertation. Heidelberg; 2015.

Berning M, Prätzel-Wunder S, Bickenbach JR, Boukamp P. Three-dimensional in vitro skin and skin cancer models based on human fibroblast-derived matrix. Tissue Eng Part C Methods 2015;21:958–70.

Boehnke K, Falkowska-Hansen B, Stark HJ, Boukamp P. Stem cells of the human epidermis and their niche: composition and function in epidermal regeneration and carcinogenesis. Carcinogenesis 2012;33:1247–58.

Boehnke K, Mirancea N, Pavesio A, Fusenig NE, Boukamp P, Stark HJ. Effects of fibroblasts and microenvironment on epidermal regeneration and tissue function in long-term skin equivalents. Eur J Cell Biol 2007;86:731–46.

Bordea C, Wojnarowska F, Millard PR, Doll H, Welsh K, Morris PJ. Skin cancers in renal-transplant recipients occur more frequently than previously recognized in a temperate climate. Transplantation 2004;77:574–9.

Bos JD, Teunissen MB, Cairo I, Krieg SR, Kapsenberg ML, Das PK, et al. T-cell receptor gamma delta bearing cells in normal human skin. J Invest Dermatol 1990;94:37–42.

Boukamp P, Petrussevska RT, Breitkreutz D, Hornung J, Markham A, Fusenig NE. Normal keratinization in a spontaneously immortalized aneuploid human keratinocyte cell line. J Cell Biol 1988;106:761–71.

Brown S, Pineda CM, Xin T, Boucher J, Suozzi KC, Park S, et al. Correction of aberrant growth preserves tissue homeostasis. Nature 2017;548:334–7.

Chodaczek G, Papanna V, Zal MA, Zal T. Body-barrier surveillance by epidermal γδ TCRs. Nat Immunol 2012;13:272–82.

Cordova A, Toia F, La Mendola C, Orlando V, Meraviglia S, Rinaldi G, et al. Characterization of human γδ T lymphocytes infiltrating primary malignant melanomas. PLoS One 2012;7:e49878.

Cruz MS, Diamond A, Russell A, Jameson JM. Human αβ and γδ T cells in Skin Immunity and Disease. Front Immunol 2018;9:1304.

Dalessandri T, Crawford G, Hayes M, Castro Seoane R, Strid J. IL-13 from intraepithelial lymphocytes regulates tissue homeostasis and protects against carcinogenesis in the skin. Nat Commun 2016;7:12080.

Davey MS, Willcox CR, Baker AT, Hunter S, Willcox BE. Recasting human Vδ1 lymphocytes in an adaptive role. Trends Immunol 2018;39:446–59.

Davies D, Kamdar S, Woolf R, Zlatareva I, Iannitto ML, Morton C, et al. PD-1 defines a distinct, functional, tissue-adapted state in Vδ1^{+} T cells with implications for cancer immunotherapy. Nat Cancer 2024;5:420–32.

Ebert LM, Meuter S, Moser B. Homing and function of human skin gammadelta T cells and NK cells: relevance for tumor surveillance. J Immunol 2006;176:4331–6.

Elbe A, Foster CA, Stingl G. T-cell receptor alpha beta and gamma Delta T cells in rat and human skin–are they equivalent? Semin Immunol 1996;8:341–9.

Fischer S, Gesierich S, Griemert B, Schänzer A, Acker T, Augustin HG, et al. Extracellular RNA liberates tumor necrosis factor-alpha to promote tumor cell trafficking and progression. Cancer Res 2013;73:5080–9.

Gentles AJ, Newman AM, Liu CL, Bratman SV, Feng W, Kim D, et al. The prognostic landscape of genes and infiltrating immune cells across human cancers. Nat Med 2015;21:938–45.

Girard P, Charles J, Cluzel C, Degeorges E, Manches O, Plumas J, et al. The features of circulating and tumor-infiltrating γδ T cells in melanoma patients display critical perturbations with prognostic impact on clinical outcome. Oncoimmunology 2019;8:1601483.

Gjersvik P, Falk RS, Roscher I, Rizvi SMH, Mjøen G, Gude E, et al. Rates of second tumor, metastasis, and death from cutaneous squamous cell carcinoma in patients with and without transplant-associated immunosuppression. JAMA Dermatol 2023;159:923–9.

Griffith JW, Sokol CL, Luster AD. Chemokines and chemokine receptors: positioning cells for host defense and immunity. Annu Rev Immunol 2014;32:659–702.

Holling TM, Schooten E, van Den Elsen PJ. Function and regulation of MHC class II molecules in T-lymphocytes: of mice and men. Hum Immunol 2004;65:282–90.

Huth L, Amann PM, Marquardt Y, Jansen M, Baron JM, Huth S. Understanding the impact of risankizumab on keratinocyte-derived IL-23A in a novel organotypic 3D skin model containing IL-23A responsive and IL-17A producing γδ-T-cells. Cutan Ocul Toxicol 2024;43:124–8.

Jameson J, Havran WL. Skin gammadelta T-cell functions in homeostasis and wound healing. Immunol Rev 2007;215:114–22.

Jameson J, Ugarte K, Chen N, Yachi P, Fuchs E, Boismenu R, et al. A role for skin gammadelta T cells in wound repair. Science 2002;296:747–9.

Jelenčić V, Lenartić M, Wensveen FM, Polić B. NKG2D: a versatile player in the immune system. Immunol Lett 2017;189:48–53.

Jonason AS, Kunala S, Price GJ, Restifo RJ, Spinelli HM, Persing JA, et al. Frequent clones of p53-mutated keratinocytes in normal human skin. Proc Natl Acad Sci USA 1996;93:14025–9.

Lehman TA, Modali R, Boukamp P, Stanek J, Bennett WP, Welsh JA, et al. p53 mutations in human immortalized epithelial cell lines. Carcinogenesis 1993;14:833–9.

Lo Presti E, Toia F, Oieni S, Buccheri S, Turdo A, Mangiapane LR, et al. Squamous Cell Tumors Recruit γδ T cells Producing either IL17 or IFN-gamma Depending on the Tumor Stage. Cancer Immunol Res 2017;5:397–407.

MacLeod AS, Havran WL. Functions of skin-resident γδ T cells. Cell Mol Life Sci 2011;68:2399–408.

Madan V, Lear JT, Szeimies RM. Non-melanoma skin cancer. Lancet 2010;375:673–85.

Marshall AS, Silva JR, Bannerman CA, Gilron I, Ghasemlou N. Skin-Resident γδ T cells exhibit site-specific morphology and activation states. J Immunol Res 2019;2019:9020234.

Martincorena I, Roshan A, Gerstung M, Ellis P, Van Loo P, McLaren S, et al. Tumor evolution. High burden and pervasive positive selection of somatic mutations in normal human skin. Science 2015;348:880–6.

Melandri D, Zlatareva I, Chaleil RAG, Dart RJ, Chancellor A, Nussbaumer O, et al. The γδTCR combines innate immunity with adaptive immunity by utilizing spatially distinct regions for agonist selection and antigen responsiveness. Nat Immunol 2018;19:1352–65.

Michielon E, López González M, Burm JLA, Waaijman T, Jordanova ES, de Gruijl TD, et al. Micro-environmental cross-talk in an organotypic human melanoma-in-skin model directs M2-like monocyte differentiation via IL-10. Cancer Immunol Immunother 2020;69:2319–31.

Moon S, Kim DH, Shin JU. In vitro models mimicking immune response in the skin. Yonsei Med J 2021;62:969–80.

Muffler S, Stark HJ, Amoros M, Falkowska-Hansen B, Boehnke K, Bühring HJ, et al. A stable niche supports long-term maintenance of human epidermal stem cells in organotypic cultures. Stem Cells 2008;26:2506–15.

Nguyen AV, Soulika AM. The dynamics of the skin's immune system. Int J Mol Sci 2019;20:1811.

Nielsen MM, Dyring-Andersen B, Schmidt JD, Witherden D, Lovato P, Woetmann A, et al. NKG2D-dependent activation of dendritic epidermal T cells in contact hypersensitivity. J Invest Dermatol 2015;135:1311–9.

Ouwehand K, Spiekstra SW, Waaijman T, Scheper RJ, de Gruijl TD, Gibbs S. Technical advance: Langerhans cells derived from a human cell line in a full-thickness skin equivalent undergo allergen-induced maturation and migration. J Leukoc Biol 2011;90:1027–33.

Pang DJ, Neves JF, Sumaria N, Pennington DJ. Understanding the complexity of γδ T-cell subsets in mouse and human. Immunology 2012;136:283–90.

Pavez Loriè E, Boukamp P. Methods in cell biology: cell-derived matrices. Methods Cell Biol 2020;156:309–32.

Qu G, Wang S, Zhou Z, Jiang D, Liao A, Luo J. Comparing Mouse and Human Tissue-Resident γδ T cells. Front Immunol 2022;13:891687.

Ratushny V, Gober MD, Hick R, Ridky TW, Seykora JT. From keratinocyte to cancer: the pathogenesis and modeling of cutaneous squamous cell carcinoma. J Clin Invest 2012;122:464–72.

Raverdeau M, Cunningham SP, Harmon C, Lynch L. Γδ T cells in cancer: a small population of lymphocytes with big implications. Clin Transl Immunology 2019;8:e01080.

Rheinwald JG, Beckett MA. Tumorigenic keratinocyte lines requiring anchorage and fibroblast support cultured from human squamous cell carcinomas. Cancer Res 1981;41:1657–63.

Samten B. CD52 as both a marker and an effector molecule of T cells with regulatory action: identification of novel regulatory T cells. Cell Mol Immunol 2013;10:456–8.

Sanz M, Mann BT, Ryan PL, Bosque A, Pennington DJ, Hackstein H, et al. Deep characterization of human γδ T cell subsets defines shared and lineage-specific traits. Front Immunol 2023;14:1148988.

Scheurer J, Sauer B, Focken J, Giampetraglia M, Jäger A, Schürch CM, et al. Histological and functional characterization of 3D human skin models

mimicking the inflammatory skin diseases psoriasis and atopic dermatitis. Dis Model Mech 2024;17:dmm050541.

Schindelin J, Arganda-Carreras I, Frise E, Kaynig V, Longair M, Pietzsch T, et al. Fiji: an open-source platform for biological-image analysis. Nat Methods 2012;9:676–82.

Sobel K, Tham M, Stark HJ, Stammer H, Prätzel-Wunder S, Bickenbach JR, et al. Wnt-3a-activated human fibroblasts promote human keratinocyte proliferation and matrix destruction. Int J Cancer 2015;136:2786–98.

Stark HJ, Boehnke K, Mirancea N, Willhauck MJ, Pavesio A, Fusenig NE, et al. Epidermal homeostasis in long-term scaffold-enforced skin equivalents. J Investig Dermatol Symp Proc 2006;11:93–105.

Stark HJ, Willhauck MJ, Mirancea N, Boehnke K, Nord I, Breitkreutz D, et al. Authentic fibroblast matrix in dermal equivalents normalises epidermal histogenesis and dermoepidermal junction in organotypic co-culture. Eur J Cell Biol 2004;83:631–45.

Strid J, Tigelaar RE, Hayday AC. Skin immune surveillance by T cells–a new order? Semin Immunol 2009;21:110–20.

Sumaria N, Roediger B, Ng LG, Qin J, Pinto R, Cavanagh LL, et al. Cutaneous immunosurveillance by self-renewing dermal gammadelta T cells. J Exp Med 2011;208:505–18.

Temchura VV, Frericks M, Nacken W, Esser C. Role of the aryl hydrocarbon receptor in thymocyte emigration in vivo. Eur J Immunol 2005;35: 2738–47.

Tham M, Stark HJ, Jauch A, Harwood C, Pavez Lorie E, Boukamp P. Adverse effects of vemurafenib on skin integrity: hyperkeratosis and skin cancer initiation due to altered MEK/ERK-signaling and MMP activity. Front Oncol 2022;12:827985.

Toia F, Di Stefano AB, Meraviglia S, Lo Presti E, Pirrello R, Rinaldi G, et al. Γδ T cell-based immunotherapy in melanoma: state of the art, 2019. J Oncol; 2019:9014607.

Toulon A, Breton L, Taylor KR, Tenenhaus M, Bhavsar D, Lanigan C, et al. A role for human skin-resident T cells in wound healing. J Exp Med 2009;206:743–50.

van den Bogaard EH, Tjabringa GS, Joosten I, Vonk-Bergers M, van Rijssen E, Tijssen HJ, et al. Crosstalk between keratinocytes and T cells in a 3D microenvironment: a model to study inflammatory skin diseases. J Invest Dermatol 2014;134:719–27.

Vantourout P, Hayday A. Six-of-the-best: unique contributions of γδ T cells to immunology. Nat Rev Immunol 2013;13:88–100.

Wang YN, Lee HH, Jiang Z, Chan LC, Hortobagyi GN, Yu D, et al. Ribonuclease 1 Enhances antitumor Immunity against Breast Cancer by Boosting T cell Activation. Int J Biol Sci 2023;19:2957–73.

Wensveen FM, Jelenčić V, Polić B. NKG2D: a master regulator of immune cell responsiveness. Front Immunol 2018;9:441.

Whitfield ML, George LK, Grant GD, Perou CM. Common markers of proliferation. Nat Rev Cancer 2006;6:99–106.

Wrobel P, Shojaei H, Schittek B, Gieseler F, Wollenberg B, Kalthoff H, et al. Lysis of a broad range of epithelial tumour cells by human gamma Delta T cells: involvement of NKG2D ligands and T-cell receptor- versus NKG2D-dependent recognition. Scand J Immunol 2007;66:320–8.

Wu Y, Biswas D, Usaite I, Angelova M, Boeing S, Karasaki T, et al. A local human Vδ1 T cell population is associated with survival in nonsmall-cell lung cancer. Nat Cancer 2022;3:696–709.

Xiang J, Qiu M, Zhang H. Role of dendritic epidermal T cells in cutaneous carcinoma. Front Immunol 2020;11:1266.

This work is licensed under a Creative Commons Attribution-NonCommercial-NoDerivatives 4.0 International License. To view a copy of this license, visit http://creativecommons.org/licenses/by-nc-nd/4.0/